A Simulation Tool for Interference Analysis in MIMO Wavelength Division LiFi Indoor Networks

Giovanni Luca Martena
pureLiFi Ltd.
Edinburgh, UK
gianluca.martena@purelifi.com

Janis Sperga
pureLiFi Ltd.
Edinburgh, UK
janis.sperga@purelifi.com

Dayrene Frometa Fonseca
IMDEA Networks Institute
Madrid, Spain
dayrene.frometa@imdea.org

Rui Bian
pureLiFi Ltd.
Edinburgh, UK
rui.bian@purelifi.com

Borja Genovés Guzmán
IMDEA Networks Institute
Madrid, Spain
borja.genoves@imdea.org

Mohamed Sufyan Islim
pureLiFi Ltd.
Edinburgh, UK
mohamed.islim@purelifi.com

John Kosman
pureLiFi Ltd.
Edinburgh, UK
john.kosman@purelifi.com

Harald Haas
pureLiFi Ltd.
Edinburgh, UK
harald.haas@purelifi.com

***Abstract*—In this paper we propose a novel simulation tool for indoor Light Fidelity (LiFi) networks based on Wavelength Division (WD) with real optical filters characteristics. Firstly we present the measured passband spectra of optical filters, along with a system model validation relying on such acquired spectra. Secondly, we propose a simulation tool developed to extend the work of adaptive wavelength division multiple access to the multiple-input multiple-output case, suitable for conducting Monte Carlo simulations. Then, we validate such tool by considering an example scenario with fixed positions and orientations, including increasing number of users in an indoor LiFi network using WD. In order to better clarify the interference contributions to the quality of service provided, we consider the first user as reference, and evaluate how the presence of progressively higher number of users in its vicinity impacts the interference that the main user is experiencing. We then analyse how the signal-to-interference-plus-noise ratio, interference-to-noise ratio and signal-to-interference ratio figures of the main user change depending on how many interfering users are included in the considered scenario.**

***Index Terms*—inter-user interference, LiFi, optical filters, wavelength division**

I. Introduction

As reported, the global demand for high speed wireless data keeps increasing and forecasts show that there will be 5.7 billions of connected mobile devices by 2023 [1]. The radio frequency (RF) technology is commonly used to satisfy these demands, but it may not be sufficient anymore in the near future. On the other hand, Optical Wireless Communications (OWC) and Light Fidelity (LiFi) [2], which is its networked counterpart, are now mature enough technologies to be seen as a viable complement to RF. This is because part of the data traffic can be securely offloaded to LiFi networks, which uses the visible light and near infrared spectra and thus avoids all interference with common RF technologies [3]. Thanks to the improved capacity introduced, and the absence of interference with RF, LiFi also gives space to other technologies like the Internet of Things (IoT) [4]–[10] which require an even higher number of connected devices. In OWC a light source is used to transmit a signal in the optical domain, by modulating its intensity according to the employed modulation scheme. At the receiver side, a photodetector (PD) is acting as a transducer from the optical to the electrical domain. In fact, these devices (i.e. PIN photodiodes, avalanche photodiodes, single photon avalanche diodes) output a current flow which is proportional to the amount of light impinging on the PD. This current can then be amplified and converted in voltage with a transimpedance amplifier (TIA), and the original signal can be reconstructed and demodulated [11].

In a system based on wavelength division (WD), a thin-film optical filter is mounted in front of the PD to improve channel separation. In fact, Red-Green-Blue-Amber (RGBA) Light Emitting Diodes (LEDs) are used in WD systems in place of regular phosphor-coated white lighting fixtures. This has two notable advantages: firstly, as the use of phosphors introduces a response delay in regular lighting fixtures, RGBA LEDs can achieve a much higher data rate. Secondly, since each individual LED inside the RGBA fixture can be addressed individually, they form independent parallel channels. Combining both these advantages, WD systems have the potential of achieving very high transmission speeds with respect to regular single colour networks [12]. One of the challenges of WD systems comes with user mobility. The work in [13] tackles user mobility in LiFi. In fact, the authors have conducted an experiment to sample the orientation of real users, and the polar angle (the inclination with respect to the floor) at which their mobile devices were being held. This data has then been well fitted with a Gaussian distribution for the polar angle and a uniform distribution for the orientation, in the case of walking users. As a direct consequence, it is unlikely that the light from a fixture acting as an Access Point (AP) in a LiFi network will always arrive at the PD of a mobile device with an angle of incidence (AoI) of 0°. Thus, the spectral characteristic (i.e., the transmissivity curve) of the optical filter will suffer from two concurrent effects as the AoI increases: the central wavelength (CWL) of the optical filter will shift towards shorter wavelengths, and the shape

of the filter's passband will degrade, lowering both the width and the peak of the transmissivity curve. The work in [14] describes both effects. However, a mathematical equation is only given for the first effect, the passband shift. It allows, given a starting CWL for the optical filter's passband, to calculate what the shifted CWL will be at any given AoI. With this framework in mind, the work in [15] proposes a new scheduling scheme (i.e. a resource allocation scheme) that is able to limit the interference in an indoor WD-based LiFi network while accounting for and adapting to user mobility. This is referred to as Adaptive wavelength division multiple access (WDMA), and is compared to a fixed scheduling scheme (thereby referred to as Classic WDMA). Additionally, the work in [16] provides a mathematical framework and system design insights for such networks. In [17], the authors present a simulation tool for a WiFi/LiFi hybrid network solution. However, a TDMA multiuser access implementation is used for LiFi, which considerably reduces network performances with respect to WDMA because the time resource is shared among all users. To the best of the authors' knowledge, the contributions of this paper are hereby summarised. Firstly, we characterise 4 optical filters at increasing AoIs, to investigate their spectral degradation. Then we validate the model used throughout this work by comparing theoretical and measured power reception. Secondly, we extend the scheduling scheme in [15] to the Multiple-Input Multiple-Output (MIMO) scenario, and develop a simulation tool that can be used to carry out estimations with the Monte Carlo method. Network data rate, both aggregate and per user, and connection loss probability for a chosen number of users can be estimated in this way. This tool employs the measured optical filters spectra for increased accuracy with respect to ideal optical filters. Finally, we analyse the interference of a single user in a specific scenario with an increasing number of interfering users, until the interference is maximised (i.e. all APs in the field of view of the main user are transmitting to other users).

The rest of the paper is organised as follows: in Section II, the related system model is introduced. In Section III, the LiFi indoor scenario adopted is discussed. In Section IV, all results are presented and discussed. Finally, conclusions are drawn in Section V.

II. System Model

We use the widely adopted equation proposed in [18] for the free-space optical path loss of a Lambertian source:

$$H(0)_{\mathrm{DC}} = \frac{(m+1)}{2\pi d^2}\cos(\phi)^{m-1} A(\psi)_{\mathrm{eff}}, \tag{1}$$

where m is the Lambertian emission order of the emitted light beam, d is the Euclidean distance between the transmitter and the receiver, ϕ and ψ are the transmitter emission angle and receiver AoI respectively, and $A(\psi)_{\mathrm{eff}}$ is the effective active area of the receiver. It is possible to define the Lambertian emission order as:

$$m = -\frac{\ln 2}{\ln \cos \phi_{1/2}}, \tag{2}$$

where $\phi_{1/2}$ is the half emission angle of the transmitter. The receiver effective area can be defined as:

$$A(\psi)_{\mathrm{eff}} = A_{\mathrm{det}} G_{\mathrm{OC}} \cos(\psi)\mathrm{rect}(\psi), \tag{3}$$

where A_{det} is the detector area, G_{OC} is the gain of an optical concentrator and $\mathrm{rect}(\psi)$ is a rectangular function that allows to factor the effect of its Field of View (FOV), defined as:

$$\mathrm{rect}(\psi) = \begin{cases} 1 & \text{if } \psi \leq \psi_{\mathrm{FOV}} \\ 0 & \text{in all other cases,} \end{cases} \tag{4}$$

where ψ_{FOV} is the concentrator FOV. At this point, it is possible to write the equation for the average optical power that hits the external layer of the optical filter put in front of the receiver:

$$P_{\mathrm{rx}}^{\mathrm{opt}} = P_{\mathrm{tx}}^{\mathrm{opt}} H(0)_{\mathrm{DC}}, \tag{5}$$

where $P_{\mathrm{tx}}^{\mathrm{opt}}$ is the average transmitted optical power. From here, we formulate the expression for electrical current generated after the PD as:

$$I_{\mathrm{rx}} = P_{\mathrm{rx}}^{\mathrm{opt}} \int_{\alpha}^{\beta} S_{\mathrm{tx}}(\lambda) T_{\mathrm{OF}}(\lambda) R(\lambda) \mathrm{d}\lambda, \tag{6}$$

where $S_{\mathrm{tx}}(\lambda)$ is the normalised transmitter emission spectrum, $T_{\mathrm{OF}}(\lambda)$ is the transmission characteristic of the optical filter before the PD, $R(\lambda)$ is the responsivity of the PD, and α and β are respectively the lower and upper limit of the considered wavelength range (set as $\alpha = 400$ nm and $\beta = 700$ nm in this paper). It also has to be noted that each PD is simultaneously hit by the light beams coming from every active transmitter in range other than the one delivering the useful signal, resulting in an interference component in the generated electrical signal.

If I_{sig} is the average electrical current generated by the desired signal component, I_{int} the one generated from the interference, and I_{noise} the one generated as a result of noise contributions (thermal and background light), it is possible to write the expression of the electrical signal-to-interference-plus-noise ratio (SINR) measured after the TIA:

$$\gamma_{\mathrm{SINR}} = \frac{(I_{\mathrm{sig}} G_{\mathrm{TIA}})^2}{[\mathrm{var}(I_{\mathrm{noise}} G_{\mathrm{TIA}}) + \mathrm{var}(I_{\mathrm{int}} G_{\mathrm{TIA}})]}, \tag{7}$$

where G_{TIA} is the gain of the TIA. It is then possible to define the signal-to-noise ratio (SNR), the interference-to-noise ratio (INR) and the signal-to-interference ratio (SIR) in the same manner:

$$\gamma_{\mathrm{SNR}} = \frac{(I_{\mathrm{sig}} G_{\mathrm{TIA}})^2}{\mathrm{var}(I_{\mathrm{noise}} G_{\mathrm{TIA}})}, \tag{8}$$

$$\gamma_{\mathrm{INR}} = \frac{\mathrm{var}(I_{\mathrm{int}})}{\mathrm{var}(I_{\mathrm{noise}})}, \tag{9}$$

and

$$\gamma_{\mathrm{SIR}} = \frac{(I_{\mathrm{sig}} G_{\mathrm{TIA}})^2}{\mathrm{var}(I_{\mathrm{int}} G_{\mathrm{TIA}})}, \tag{10}$$

Finally, as shown in [14], the shifted CWL of an optical filter, $\lambda_{\mathrm{OF}}(\psi)$, can be formulated as:

$$\lambda_{\mathrm{OF}}(\psi) = \lambda_{\mathrm{OF}}(\psi = 0)\sqrt{1 - \frac{\sin^2(\psi)}{n_{\mathrm{e}}^2}}, \tag{11}$$

where ψ is the AoI of the impinging light, $\lambda_{\mathrm{OF}}(\psi = 0)$ is the CWL of the considered transmission spectrum when the light hits the receiver perpendicularly, and n_{e} is the effective refractive index of the specific optical filter employed.

III. Indoor LiFi Network Scenario

A. Extension to the MIMO case

In this work we refer to the scheduling scheme presented in [15], in which each user is assigned 1 WD channel based on highest SNR. This proved to substantially increase the network's average data rate with respect to a fixed allocation scheme, while also lowering all users' connection loss probability. However, while these benefits cannot be denied, large portions of the network's capabilities still remain untapped especially when user density is low. This is a fundamental limitation that can be overcome by adding an additional step after every user has been served with at least 1 channel. In this step, channels continue to be allocated with highest SNR, until either every user has been served with the maximum amount of channels allowed by their front end (4 in the case of RGBA), or every transmitter in each user's sight has already been allocated. In this way the network will be able to better serve users with more favourable conditions, while still being able to provide basic services to users with low spatial diversity between them. In this work, we have developed a simulation tool (based on the provided system model) able to estimate the results in terms of network maximum, average and per user data rate, and connection loss probability. This tool can simulate a scenario with variable room dimensions and AP arrangements, and is based on the Monte Carlo method. Furthermore, we use this tool to examine a particular case (described in the next subsection) with an increasing number of users.

B. Example scenario

This paper considers a square room that is 6 m long, 6 m wide, and 3 m high. fitted with 25 RGBA LiFi APs on the ceiling. Thus, each AP is made up of 4 coloured LEDs, each emitting up to 3.2 W of optical power. In this way, considering a common efficiency value for LEDs $\eta = 90$ lm/W, the room also benefits from adequate illumination for most tasks. The room size in this example has been chosen to represent an arbitrarily large space accommodating a high number of users. The number of APs has been chosen so that they are close enough to provide uniform illumination and replicate common situations regarding offices and meeting rooms. If other arrangements are desirable, even with rectangular rooms rather than square, all these parameters can be changed in the simulator. In this room, 5 concurrent users are introduced gradually and placed at specific positions and orientations. Additionally, their mobile devices are being held at specific inclinations. Table I and Fig. 1 give a summary of the geometric positioning for each user. These positions and orientations have been specifically chosen to represent an indoor scenario that is both likely to happen in a real use case, and compatible with the user mobility statistics reported in [13].

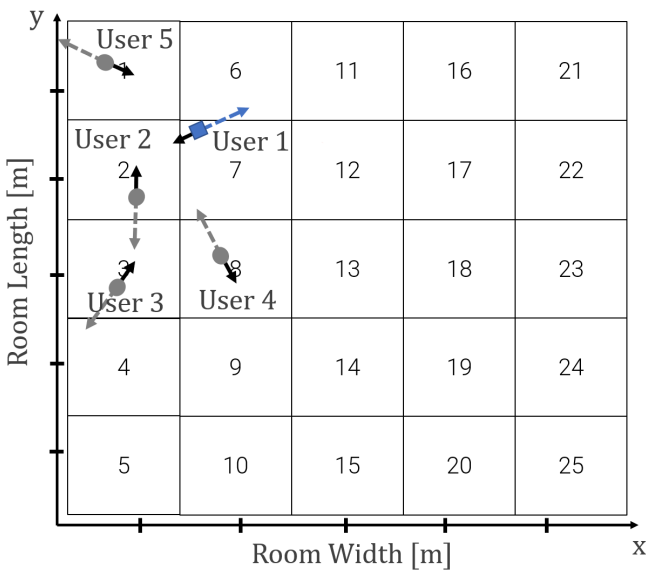

Fig. 1. Indoor LiFi Network Scenario. The room dimensions are 6x6x3 m. It includes 5 users, where user 1 (main) is a blue square while the other users (interfering) are depicted as gray circles. Each user has a solid black arrow showing the orientation of the device they are holding, while the dashed and coloured arrows (blue and grey) indicate the users' orientation in space. While walking, users are facing their devices in order to see the screens. The receivers in turn, being fixed on the screen, are facing the opposite direction.

User 1 will be referred to as the "main" user, and we will observe how the interference experienced by said user grows and evolves as the room is filled with other users (n. 2 - 5), referred to as "interfering" users.

TABLE I
Users' Geometric Parameters

User	*Location*	*Orientation*	*Inclination*
User 1 (main)	$[1.60, 4.40, 1]$	$76°$	$23°$
User 2 (interfering)	$[0.93, 3.87, 1]$	$180°$	$32°$
User 3 (interfering)	$[0.47, 2.87, 1]$	$210°$	$19°$
User 4 (interfering)	$[0.47, 5.33, 1]$	$300°$	$32°$
User 5 (interfering)	$[1.67, 3.07, 1]$	$330°$	$24°$

Each mobile device is equipped with 4 independent LiFi receivers, each of those fitted with a differently coloured optical filter to comply with the WD paradigm.

As more users are added to the room, the main user will experience interference from all APs in his field of view. In addition, he will experience cross-talk interference from the channels assigned to himself, due to spectral leakage. Relevant system parameters are summarised in Table II.

IV. Results and Discussion

A. Optical Filters characterisation

In this section we present the results of the experimental characterisation of 4 optical filters made by Thorlabs, whose model are: Blue, FB450-40; Green, FB550-40; Amber, FB590-10; Red, FB650-40. The objective is to investigate their transmission characteristics with an increasing AoI of the

TABLE II
SIMULATION PARAMETERS

Symbol	**Description**	*Value*
$[X, Y]$	Room width and length	6 m
h	Room height	3 m
d'	Inter-AP distance	1.2 m
P_{LED}	Emitted Optical Power from single colour LED	3.2 W
A_{det}	Single detector area	7.07 mm^2
N_{PD}	Number of detectors per receiver	2
Ψ_{c}	Receiver half Field of View	40°
G_{c}	Optical Concentrator Gain	2.25
G_{TIA}	Transimpedance amplifier Gain	2000 V/A

impinging light. Such curves are also used in the simulation tool, and were obtained experimentally with a spectrometer, which captures the wavelength-dependent distribution of emitted power from an optical source (i.e. its emissivity). Additionally, once the emissivity has been acquired, it is possible to obtain the transmissivity of an optical filter interposed between the source and the spectrometer, by means of a subtraction algorithm included in the spectrometer software. The spectral characteristics have been acquired in a dark environment (to avoid interference from background illumination) at increasing AoI, starting at 0° up to 40°, with an acquisition made every 5°. In this experiment, only the optical filters were rotated of the intended quantity while leaving the spectrometer at an AoI = 0°. In this way, the optical path loss remains unchanged throughout the whole experiment. Fig. 2 shows the results of the characterisation, plotted with the relevant LED normalised spectrum as a reference. The most important thing to note is that, especially at higher AoIs, there is a non-negligible difference both with respect of an ideal rectangular shape usually assumed for optical filters, but also of curves found in datasheets. This means that, wherever possible, a similar characterisation of the employed optical filters should be conducted even in works entirely based on simulations, so that the end results are closer to reality. This is still an open challenge, as past literature gives precise indications only regarding what is to be expected in terms of CWL shift. On the contrary, given an optical filter, it is not easy to foresee what the spectral degradation will be with respect to the AoI, as detailed information on the internal structure of the individual filter would be required. Obtaining such knowledge about optical filters is a challenge for two reasons. Firstly, details about construction of the optical filters are part of the manufacturers' intellectual property, and are not easily accessible in normal circumstances. Secondly, a spectral degradation model derived in this way would only be specific to the particular optical filter model considered, and only if a large number of samples of the same optical filter are tested in order to rule out the impact of high variability between samples. In the next section of this work, the measured transmissivity curves have been applied to all users. In order to validate the system model adopted in the simulations, we have used a similar experimental setup, using a power meter instead of a spectrometer. A RGBA LED optical source is

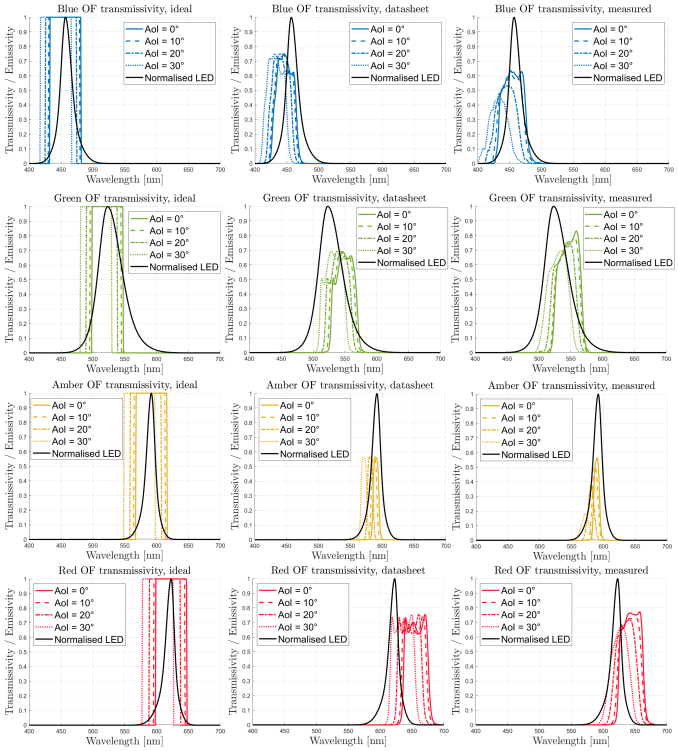

Fig. 2. Optical filters comparison. Each row contains ideal, datasheet and measured spectra for each colour. At higher AoIs, the optical filters' characteristics show a shift towards shorter wavelengths. However, only measured spectra also report substantial spectral degradation. Conversely, ideal and datasheet curves have no reliable information on this effect.

placed at a fixed distance from the power meter, and an optical filter is interposed between the two. In order to rule out cross-talk between colours due to spectral leakage, only one of the coloured LEDs is active at any given time. The optical filter (of the same colour as the LED source) can be rotated as before, and the received power has been acquired at AoI = 0°, 10°, 20° and 30°. These acquisitions were made in a dark environment, and have been compared with the theoretical values, using the same measured optical filters characteristics. A close match between experimental and theoretical data can be appreciated in Fig. 3 in the next page. It is important to note that, given all earlier considerations, using ideal characteristics for optical filters (or even the ones taken from the datasheet) would have yielded inaccurate results compared with actual devices.

B. Interference Analysis

This analysis is carried out with respect to a specific scenario as outlined in Section IIIb, with users taking a fixed position and orientation in space, which is compatible with user mobility statistics. It should be noted that observing a single fixed scenario does not provide enough insight to draw general conclusions. Nonetheless, we carry it out as a validation for the tool detailed in Section IIIa, so that future works can be conducted with confidence that its results are trustworthy. Given the aforementioned location-related and

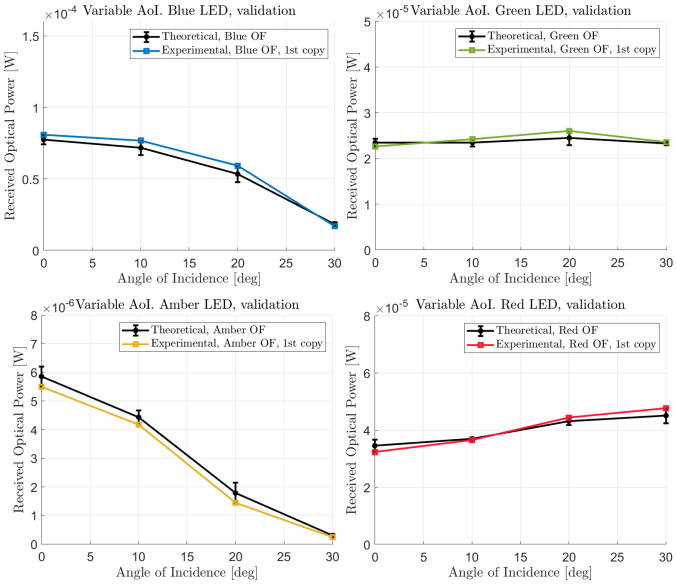

Fig. 3. Measured VS Theoretical received power. A close match between experimental and theoretical is obtained by using measured optical filters spectra, which also account for the spectral degradation at higher AoIs.

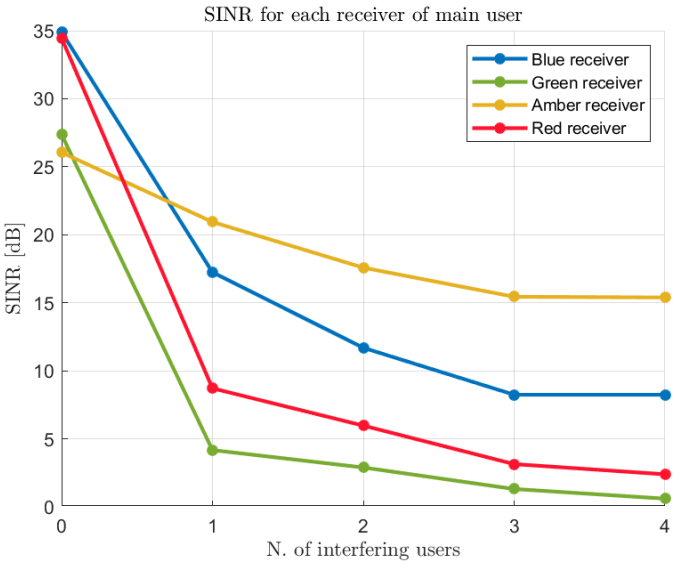

Fig. 4. SINR of the main user for increasing interfering users.

geometric parameters for every user, the adaptive allocation procedure yields the following result. User 1 (the main user) is allocated the Blue and Amber channels from AP 2, while Green and Red from AP 7. User 2 is allocated the Blue and Amber channels from AP 1, and Green and Red from AP 2. User 3 is allocated all channels from AP 3. User 4 is allocated the Blue and Amber channels from AP 7, and Green and Red channels from AP 1. Finally, user 5 is allocated all channels from AP 8. It is important to note that in this configuration, this allocation for the main user does not change as more users are introduced. For this scenario, the SINR, INR and SIR values for each receiver of the main user, with increasing numbers of interfering users, are shown in Fig. 4, 5 and 6 respectively. In Fig. 4, we can see how the contribution to the interference introduced by the first interfering user causes a substantial drop in SINR with respect to a scenario in which no other users than the main one are present. Notably, the Amber receiver is the most robust to these changes, with SINR dropping by only 10.66 dB when the interference is at its maximum. This is because the pass band spectrum for the Amber optical filter is only 10 nm wide, and therefore more robust to interference. This is opposed to a 26.66 dB and 26.77 dB drop for the Blue and Green receivers respectively, and 32.06 dB drop for the Red receiver. Fig. 5 in the next page confirms these findings by showing how the interference grows along with the presence of interfering users. Here we can note how the Blue and Red receivers have a negative INR without other users, meaning that there is no cross-talk interference coming from other channels allocated to the main user. Conversely, both the Green and Amber receivers have positive INR even with no interfering users, because in both cases the other three active channels allocated to the main user are providing cross-talk interference. Finally, Fig. 6 in the next page shows how the signal becomes progressively weaker when compared to the interference (which, with 4 interfering users, is at its maximum for the main user). It can be inferred that for this particular case, the first interfering user (that is, user 2) is introducing the most extensive contribution to the main user's interference. This is mainly due to its position and orientation, as AP 2 (which is partly allocated to user 2), was a viable allocating option for user 1 as well. Other users are introducing a much lower contribution to the interference figure for the main user as the APs allocated to them, while still in the range of user 1, would not constitute a good allocation option for that user because of distance and AoI. Despite this, compared to using a fixed scheme based only on AP closest to the user (such as the one compared in [15]), the users have the flexibility of using more than one AP thus maximising opportunities to employ all 4 channels available to them. This is especially important for users located closer to the edge of a cell.

V. Conclusions

In this paper, we have presented the results from a characterisation of 4 optical filters, with the objective of investigating the spectral degradation generated by the light impinging at an AoI different than 0°. Results show that such degradation becomes more significant as the AoI increases. Moreover, the spectral characteristics from all filters result substantially different from the ideal rectangular shape that is usually assumed in literature. For these particular filters there is also a remarkable difference with the curves given in datasheets, and additionally, no spectral degradation information is made available. The only way of obtaining such information is by conducting a full characterisation of the specific models that are being considered, and this makes it challenging to readily obtain accurate and trustworthy results when investigating LiFi Networks that use WDMA in a user mobility

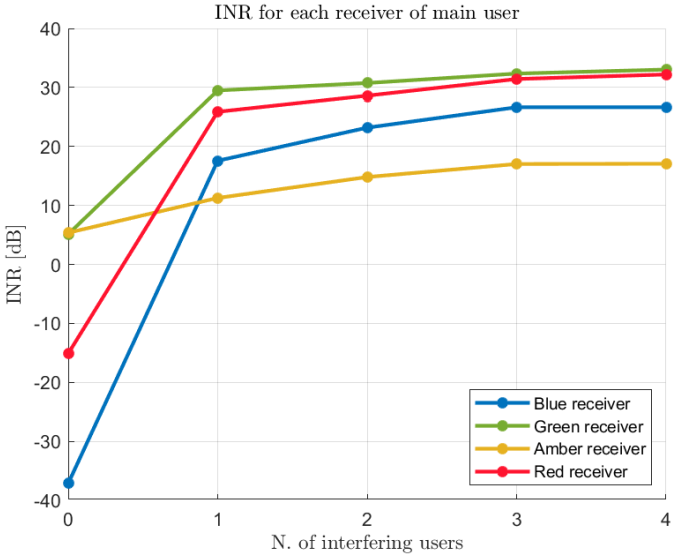

Fig. 5. INR of the main user for increasing interfering users.

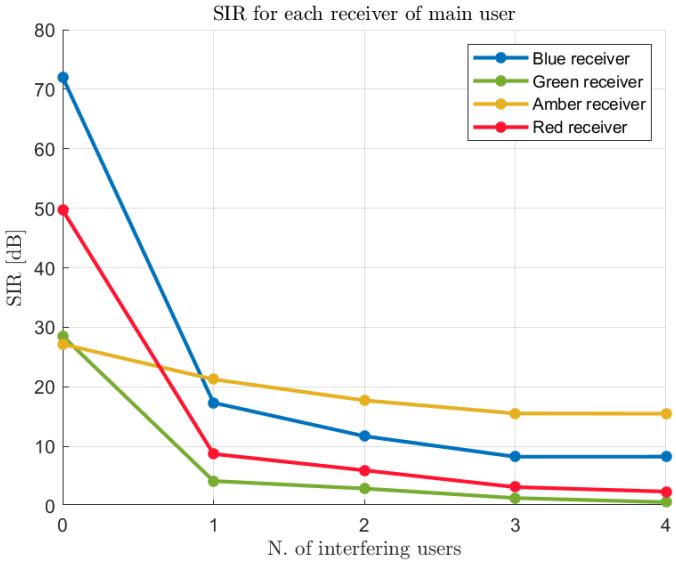

Fig. 6. SIR of the main user for increasing interfering users.

context, as the AoI of the impinging light can vary greatly. Exploring the spectral degradation for other models and other manufacturers of optical filters would be an interesting option for future works, as this particular aspect can greatly impact the performances of such systems. We have also developed and validated a simulation framework that is able to leverage the measured optical filters spectra to provide substantially more accurate results with respect to using ideal curves, or ones taken from datasheets. This tool is based on an existing scheduling scheme, which we have extended to the MIMO scenario. In fact, it was previously unable to allocate more than 1 channel per user, leaving many untapped resources in the network. To validate this tool, we have also conducted an interference analysis of a WD-based system, where 5 concurrent users were gradually added to the room and the interference for the first one monitored by means of SINR, INR and SIR curves. In future works, this framework will be used within the Monte Carlo method to evaluate network performances with an increasing numbers of users.

ACKNOWLEDGMENT

This work has been funded by the European Union's Horizon 2020 research and innovation programme under the Marie Skłodowska Curie grant agreement ENLIGHT'EM No. 814215.

REFERENCES

[1] CISCO, "Cisco annual internet report (2018-2023)." https://www.statista.com/statistics/471264/iot-number-of-connected-devices-worldwide/ CISCO, March 2020.

[2] H. Haas, L. Yin, Y. Wang, and C. Chen, "What is LiFi?," *J. Lightw. Technol.*, vol. 34, no. 6, pp. 1533–1544, 2016.

[3] X. Wu, M. D. Soltani, L. Zhou, M. Safari, and H. Haas, "Hybrid lifi and wifi networks: A survey," *IEEE Commun. Surveys Tut.*, vol. 23, no. 2, pp. 1398–1420, 2021.

[4] I. Demirkol, D. Camps-Mur, J. Paradells, M. Combalia, W. Popoola, and H. Haas, "Powering the internet of things through light communication," *IEEE Commun. Mag.*, vol. 57, no. 6, pp. 107–113, 2019.

[5] O. Alsulami, A. Alahmadi, S. Saeed, S. Mohamed, T. El-Gorashi, M. Alresheedi, and J. Elmirghani, "Optimum resource allocation in 6g optical wireless communication systems," 05 2020. © 2020 IEEE.

[6] B. Marr, "Will lifi take big data and the internet of things to a new level?." https://www.forbes.com/sites/bernardmarr/2016/01/12/will-lifi-take-big-data-and-the-internet-of-things-to-a-new-level/, 01 2016.

[7] H. Haas, J. Emlirghani, and I. White, "Optical wireless communication," *Philosophical Transactions of the Royal Society A: Mathematical Physical and Engineering Sciences*, vol. 378, no. 2169, p. 20200051, 2020.

[8] S. R. Teli, S. Zvanovec, and Z. Ghassemlooy, "Optical internet of things within 5g: Applications and challenges," in *2018 IEEE International Conference on Internet of Things and Intelligence System (IOTAIS)*, pp. 40–45, 2018.

[9] A. Gupta and X. Fernando, "Exploring secure visible light communication in next-generation (6g) internet-of-things," in *2021 International Wireless Communications and Mobile Computing (IWCMC)*, pp. 2090–2097, 2021.

[10] M. Z. Chowdhury, M. K. Hasan, M. Shahjalal, M. T. Hossan, and Y. M. Jang, "Optical wireless hybrid networks: Trends, opportunities, challenges, and research directions," *IEEE Commun. Surveys Tut.*, vol. 22, no. 2, pp. 930–966, 2020.

[11] H. Haas, M. S. Islim, C. Chen, and H. Abumarshoud, *An Introduction to Optical Wireless Mobile Communications*. 2021.

[12] R. Bian, I. Tavakkolnia, and H. Haas, "15.73 gb/s visible light communication with off-the-shelf leds," *J. Lightw. Technol.*, vol. 37, no. 10, pp. 2418–2424, 2019.

[13] M. D. Soltani, A. A. Purwita, Z. Zeng, H. Haas, and M. Safari, "Modeling the random orientation of mobile devices: Measurement, analysis and lifi use case," *IEEE Trans. on Commun.*, vol. 67, no. 3, pp. 2157–2172, 2019.

[14] J. R. Barry and J. M. Kahn, "Link design for nondirected wireless infrared communications," *Appl. Opt.*, vol. 34, pp. 3764–3776, 07 1995.

[15] G. L. Martena, R. Bian, and H. Haas, "Adaptive wdma: Improving the data rate of a densely deployed lifi network," in *Proc. of the Workshop on Internet of Lights*, IoL '21, (New York, NY, USA), p. 7–12, Association for Computing Machinery, 2021.

[16] G. L. Martena, R. Bian, and H. Haas, "Impact of passband shift in optical wireless communication systems based on wavelength division," in *ICC 2022 - IEEE International Conference on Communications*, pp. 3820–3825, 2022.

[17] S. Ullah, S. U. Rehman, and P. H. J. Chong, "A comprehensive open-source simulation framework for lifi communication," *Sensors*, vol. 21, no. 7, 2021.

[18] J. Kahn and J. Barry, "Wireless infrared communications," *Proc. of the IEEE*, vol. 85, no. 2, pp. 265–298, 1997.